SCIENTIFIC OASIS

Spectrum of Engineering and Management Sciences

Journal homepage: www.sems-journal.org
ISSN: 3009-3309

Optimization of Speckle Pattern Generation for DIC-based Mechanical Characterization of Automotive Synthetic Leathers

Vivien Nemes[1], Szabolcs Szalai[1], Brigitta Fruzsina Szívós[1], Dmytro Kurhan[2], Mykola Sysyn[3], Szabolcs Fischer[1,*]

[1] Central Campus Győr, Széchenyi István University, Győr, Hungary
[2] Department of Transport Infrastructure, Ukrainian State University of Science and Technologies, Dnipro, Ukraine
[3] Department of Planning and Design of Railway Infrastructure, Technical University Dresden, Dresden, Germany

ARTICLE INFO

Article history:
Received 25 March 2026
Received in revised form 30 May 2026
Accepted 11 July 2026
Available online 19 July 2026

Keywords:
DIC; Surface preparation and deformation measurement; Synthetic leather; Painting techniques; Speckle pattern.

ABSTRACT

Digital Image Correlation (DIC) is a pivotal non-contact technique for full-field deformation analysis in automotive engineering. However, the high flexibility and porosity of synthetic leathers often compromise speckle pattern stability and measurement accuracy. This study presents a systematic evaluation of commercial spray paints to optimize speckle pattern generation for automotive PVC and felt-based leathers. The methodology integrates standardized adhesion testing (ISO 2409 cross-cut test), drying-time optimization, and microscopic characterization to ensure robust bonding. Performance was validated through Erichsen cupping tests, simulating multi-axial strain states typical of automotive interior components. Results demonstrate that solvent-based acrylic sprays provide superior adhesion (ISO Class 0) and maintain pattern integrity under large deformations (up to 30% strain), whereas water-based alternatives suffer from cracking and delamination. The optimized painting protocol significantly reduces correlation errors and "lost subsets" in DIC software. This research provides a reliable experimental foundation for material characterization and Finite Element Method (FEM) validation of interior systems. The findings offer a practical, cost-effective framework for enhancing optical strain measurement precision in the automotive manufacturing and testing sectors.

1. Introduction

Testing the mechanical properties of textiles and synthetic leathers is an important area for the automotive industry, as these materials are essential components of interior upholstery, seat covers, and safety systems, whose durability and reliability directly affect vehicle safety, comfort, and service life. It is also important to note that these are often the first materials users encounter or come into contact with, and they often base their purchase decisions on these impressions. Thus, these

* *Corresponding author.*
E-mail address: fischersz@sze.hu

https://doi.org/10.31181/sems41202681

materials also have a direct economic impact on vehicle manufacturers, making the testing and analysis of these materials an important area of research.

Digital image correlation (DIC) is an optical measurement method that, according to the available literature, is increasingly used to examine the mechanical behavior of textiles, such as monitoring tensile or full-surface deformation. Because DIC tracks a stochastic speckle pattern applied to the surface, the quality of that pattern—its feature size, density, and grayscale (intensity) distribution relative to the correlation subset size—directly governs the matching accuracy and the resulting correlation error [1–3]. In the examination of different materials, not only mechanical characteristics but also the development of measurement and testing procedures play a decisive role [4,5]. Increasing loads and speeds require new technical and testing approaches to ensure reliability [6].

Jing *et al.* [7] examined polyurethane-coated fabric, i.e., a type of synthetic leather. The aim of the research was to map the material deformation and the local strain distribution during a uniaxial tensile test. To this end, they used the Digital Image Correlation (DIC) technique, which enabled them not only to record global force-strain curves but also to obtain a detailed picture of deformations across different zones of the material. For DIC to work, a contrasting speckle pattern must be present on the surface. The researchers therefore painted the surface of the synthetic leather textile, applying a dark, irregular pattern to a light base color.

Lomov *et al.* [8] investigated the deformation of woven textiles (e.g., glass and carbon fibers) using optical image correlation techniques (the ARAMIS system). The goal was to obtain accurate, full-surface deformation fields during various mechanical tests. Mitrovic *et al.* [9] measured the strain fields of cotton medical textiles using 2D-DIC, demonstrating the effect of fabric density.

Several studies have focused on the mechanical behavior of PVC-coated fabrics under various stresses (biaxial, uniaxial and off-axis tensile). All of them used DIC, with speckle patterns enabling tracking of the entire surface deformation [10–12]. Meyer *et al.* [13] compared real skin with artificial skin under various loads. Lee *et al.* [14] investigated the bending stress in textile-based OLEDs, validating their model with DIC measurements obtained from an artificial speckle pattern created with Duplicolor acrylic spray. The data was evaluated using ARAMIS software. Khennouf *et al.* [15] and Williams *et al.* [16] showed that for certain textiles, the natural weave pattern provides sufficient contrast, thus avoiding the need for painting [15,16].

The use of modern testing methods is essential for understanding system behavior and achieving reliable results [17,18]. DIC has proven to be an effective tool not only for examining textiles and synthetic leathers but also for characterizing the mechanical behavior of biological tissues such as skin [19].

The application of DIC technology is also evident in testing automotive fabrics, demonstrating its wide applicability. Savic *et al.* [20] investigated the mechanical behavior of various automotive seat upholstery fabrics using a uniaxial tensile test and measured total surface deformation using 2D Digital Image Correlation (DIC). The investigation also included foamed backgrounds and materials attached to a substrate. The non-contact optical measurement enabled tracking of fiber and projection direction displacements and the determination of Young's modulus, Poisson's ratio, and elongation at break. As there is currently no standardized procedure for these parameters in textiles, DIC is particularly valuable because it provides full-surface, location-based measurements of deformation. The study demonstrates that 2D DIC is a reliable method for investigating the mechanical properties of automotive interior materials, both for foam-backed and non-foam fabrics.

Several studies in literature examine automotive interior materials. One study used air permeability, abrasion resistance, and tensile strength tests to evaluate the performance of textiles and synthetic leathers using standard measurement methods [21]. The effects of the textile backing also play a significant role in the testing of synthetic leathers. One study analyzed the chemical and physical-mechanical properties of synthetic leathers reinforced with textile fabric on the back side and found that the backing layer fundamentally influences the material's tensile strength and adhesion [22]. For example, one study characterized the moisture absorption and ventilation behavior of seat fabrics using water vapor resistance and air permeability tests, supplemented by a proprietary measurement system for testing convective effects [23]. These studies highlight that the performance of textiles and synthetic leathers can be evaluated from several perspectives, including mechanical and comfort aspects, using standardized tests.

Sheilla *et al.* [24] focused on improving the surface quality of synthetic leathers, particularly protection against dirt and stains, intending to increase durability while maintaining aesthetic and comfort characteristics.

In addition to DIC technology, the literature discusses other measurement methods for textiles that reveal important properties.

Lei [25] analyzed color durability using rubbing tests, demonstrating that it is good when dry but has weaker adhesion when wet, and proposed methodological improvements to increase measurement reliability. Kumpikaitė *et al.* [26] evaluated the color fastness of linen/silk-blended fabrics after dyeing and digital printing and found excellent performance under rubbing, washing, and perspiration. According to their results, the dyes adhered permanently, and the printed fabrics exhibited less shrinkage, an advantage in processing. Wang *et al.* [27] evaluated the drying behavior of geopolymer-based coatings using standardized methods, with surface drying time determined in accordance with ISO 9117-3:2010. In contrast, the pressure-free ("print-free") drying time was determined in accordance with ISO 9117-6:2012. Nguyen *et al.* [28] applied the latter standard to examine the drying time of environmentally friendly coatings based on alkyd resin and modified with graphene oxide. Also, they used the ISO 1519:2011 standard to determine the flexural strength. Another study evaluated the degree of drying (T1) in accordance with ISO 9117-5 for a fast-drying, water-based acrylic paint (Hydrapid 1C Acrylic Paint 5482) [29]. Todorov *et al.* [30] also used the EN ISO 9117-5 standard to test alkyd resin-based coatings: the resin films were applied to glass plates, then dried in air and by heat treatment, and the degree of drying was measured using an Erichsen 415 device. Butschle *et al.* [31] analyzed the drying of coatings based on the same standard using the Bandow–Wolff method, which allows the determination of different stages (dust-free (TG1), touch-free (TG3), assembly-free (TG5)), providing an accurate picture of the temporal evolution of the industrial applicability of coatings.

The ISO 2409:2020 standard cross-cut test was used to examine the adhesion properties of coatings, as used by Hou *et al.* [32] for superhydrophobic antibacterial coatings and by Barbu *et al.* [33] for organic coatings applied to Kevlar composites. The method enables the objective classification of coating adhesion, ranging from 0 (perfect adhesion) to 5 (significant detachment).

The next part of the article continues with the Materials and Methods (Section 2), which describes the materials used, test specimens, the paints tested, the tools and standards used in the research, and the methods and procedures used. This is followed by the Results and Discussion (Section 3), which presents the test results and their interpretation. The article concludes with the Conclusions (Section 4), which summarizes the most important findings and draws conclusions.

2. Materials and Methods

The primary objective of the research was to examine the applicability of commercially available spray paints on various synthetic leathers. These surfaces were evaluated to determine the most suitable paints for DIC. This section discusses experimental raw materials, paints, measuring instruments, and the various paint testing procedures used in the research.

2.1 Specimens

During the tests, two types of synthetic leather and one type of felt were used (Table 1), each cut into 30×100 mm samples. Three test specimens were prepared for each paint, and—unless stated otherwise—every reported value represents the mean of these three repeated measurements (n = 3). Material S1 is shown in Figure 1(a), S2 in Figure 1(b) and S3 in Figure 1(c).

Table 1
Materials used for painting tests

ID	Name	Color
S1	EVA, Polyethylene	Black
S2	100% Polyester felt	Dark Green
S3	Interior door synthetic leather of the Opel Astra	Black

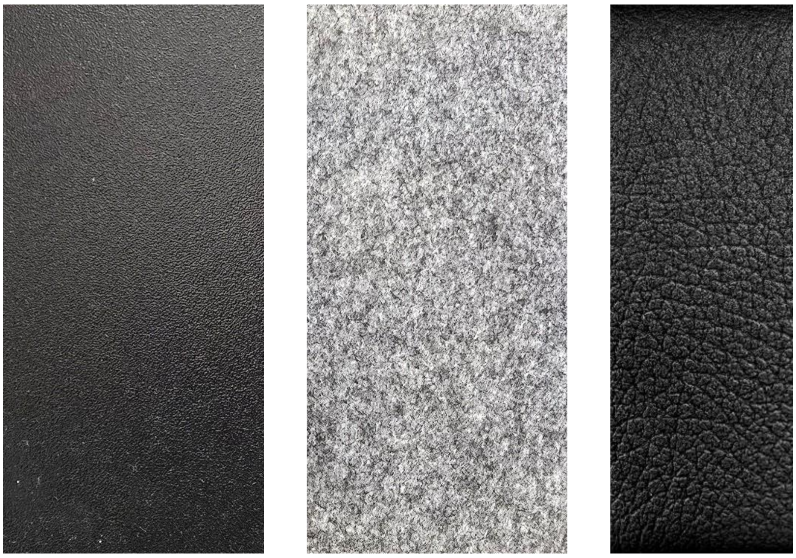

(a) **(b)** **(c)**

Fig. 1. Materials: (a) S1; (b) S2; (c) S3

2.2 Tested paints

During the tests, ten light-colored base paints (P9, P10, P12, P13, P15, P17, P18, P20, P22, P24) were tested, and six dark paints (P11, P14, P16, P19, P21, P23) were selected for the speckle pattern. The aim was to identify commercially available spray paints with high coverage. White proved to be the most suitable color for the primer paint, as it provides the greatest contrast with the dark topcoat. The following table summarizes the paints selected for testing (Table 2). The paints used are shown in Figures 2 and 3.

2.3 Surface preparation for DIC measurement, paint film thickness measurement

For digital image correlation (DIC) measurements, a high-contrast speckle pattern was created on the test surfaces. In the first step, a uniform light base coat was applied using a spray nozzle to completely cover the synthetic leather, except for P9 paint, which was applied by brush due to its packaging. Dark dots were then applied with spray paint to create a discrete, randomly distributed speckle pattern.

The thickness of the applied paint layer was determined in a wet state using an Elcometer 112Al paint thickness gauge (Figure 4), in accordance with ISO 2808:2019 (Paints and varnishes –

Determination of film thickness) [34]. After painting, the device was pressed directly into the wet layer, then lifted out, and the thickness was read from the scale in micrometers (10^{-6} m). Three measurements were taken on each test piece, and the results were averaged. The device's measuring range was 25–3000 µm.

Table 2
Applied paints

ID	Name	Producer	Color	Dispensing [ml]
P9	Fabric Paint - Machine Washable	Pentart	White	50
P10	TEXstyle spray	Dupli-Color	White	150
P11	TEXstyle spray	Dupli-Color	Black	150
P12	Chalk effect spray	Maestro	White	400
P13	Chalk spray	Pinty Plus	Broken White	400
P14	Acrylic matt paint 9004	Maestro	Black	400
P15	Acrylic matt paint 9003	Maestro	White	400
P16	Prisma Color Acryl 9005 M	Schuller	Black	400
P17	Prisma Color Acryl 9010 M	Schuller	White	400
P18	Industrial Ral Acryl spray satin matt 9010	Motip	White	400
P19	Evo Acrylic RAL 9005	Pinty Plus	Black	400
P20	Evo Matt RAL 9010	Pinty Plus	White	400
P21	Evo Matt RAL 9005	Pinty Plus	Black	400
P22	Evo Primer	Pinty Plus	White	400
P23	Home	Pinty Plus	Home Black	400
P24	Home	Pinty Plus	Foggy Blue	400

Fig. 2. Light-colored paints: P9, P10, P12, P13, P15, P17, P18, P20, P22 and P24

Fig. 3. Dark-colored paints: P11, P14, P16, P19, P21 and P23

Fig. 4. Elcometer 112Al wet film comb

2.4 Measurement Methods

The current section describes the measurement procedures used to test paints.

The Touch Test is a subjective, tactile test method designed to determine when painted test specimens are dry enough to be moved safely. After painting, the specimens should be touched at 5-minute intervals with a rubber-gloved hand and checked for any paint marks at the point of contact. If the surface still leaves a mark, the test should be repeated after another five minutes. The test specimens can be considered sufficiently dry when touching them does not cause discoloration or paint residue, so further preparation or measurement can begin without risk. The standard conditions, specified in ISO 3270 [35], are the following: atmosphere temperature 23 ± 2 °C and relative humidity of 50 ± 5 %. It is not needed to have air circulation, as it affects the drying time.

The purpose of the Print Free Test is to determine when the paint reaches a state where it can be loaded but remains flexible, i.e., does not harden completely. This is important because DIC tests require an adhesive layer that transmits the deformation of the test specimen, so a completely dry, rigid coating cannot be used.

The method is based on the ISO 9117-6:2012 and ISO 9117-5:2012 standards but is applied in a modified form with respect to the loads [36,37]. During the test, a paper disc with a diameter of 26 mm and a weight of 80 g/m^2 is placed on the painted surface, on which a rubber element with a diameter of 22 mm, a thickness of 5 mm and a hardness of 50 IRHD is placed. Weights of 20 g, 200 g, 500 g and 1000 g are placed on this in sequence, each for 60 seconds. The test specimen is then struck from a height of at least 20 mm onto a 30-mm-thick wooden surface.

If the paper does not stick to the paint, proceed to the next weight; if it does, repeat the measurement after 15 minutes. The paint passes the test if it can withstand a 1000 g load without the paper sticking to the painted surface.

It is important to note that this method evaluates only the load-bearing capacity and elasticity of the coating and does not provide information on surface adhesion, which must be verified by a separate test.

The Cross-Cut Test is a standard grid-cutting test method used to evaluate paint adhesion after grip-dry. The test is performed in accordance with ISO 2409:2020, typically using an Elcometer 107 Cross Hatch Cutter (Figure 5) with a cutting head suitable for the film thickness (e.g., 6×2 mm) [38].

During the test, six pairs of parallel scratches must be made on the coating surface, each at right angles to the others. Then, adhesive tape with the adhesion strength specified by the standard must be stuck to the grid and pulled off abruptly at a 60° angle. The aim is to determine how well the coating adheres to the substrate: after removing the adhesive, any paint detachment must be examined.

The evaluation is based on a classification system ranging from 0 to 5, as specified in the standard, where lower numbers indicate better adhesion. This test thus reliably indicates whether the painted layer can transmit the test specimen's deformation without detaching from the surface.

Fig. 5. Elcometer 107 Cross Hatch Cutter

The purpose of the Modified Bending Test is to examine the formability and adhesion of the paint layer. The procedure is based on a combination of the ISO 1519:2011 (Paints and varnishes – Bend test, cylindrical mandrel) and ISO 1518-1:2023 (Paints and varnishes – Scratch resistance) standards [39,40]. This is necessary because preliminary research has shown that, after bending, the coating may appear visually undamaged yet in fact partially detach from the substrate, thereby failing to transmit the test specimen's deformation adequately. When combined with the scratch test, this defect can be clearly detected.

Test procedure: the coating in the center of the painted test piece must be cut through to full depth with a scratch gauge, then the sample must be bent 180° using a 10 mm diameter bending roller, as shown in Figure 6. The results must be evaluated according to three categories:

1. after bending, the paint sticks along the cut, not separating from the surface;
2. flaking and minor cracking are observed along the cut line;
3. the paint is peeling along the cut or even in other areas, with insufficient adhesion.

The modified bending test should be performed at several time points: 6, 12, and 24 hours after painting, and again after the paint has completely dried, taking into account the results of the cross-cut test. Test specimens that did not perform well in previous tests should not be subjected to the bending test.

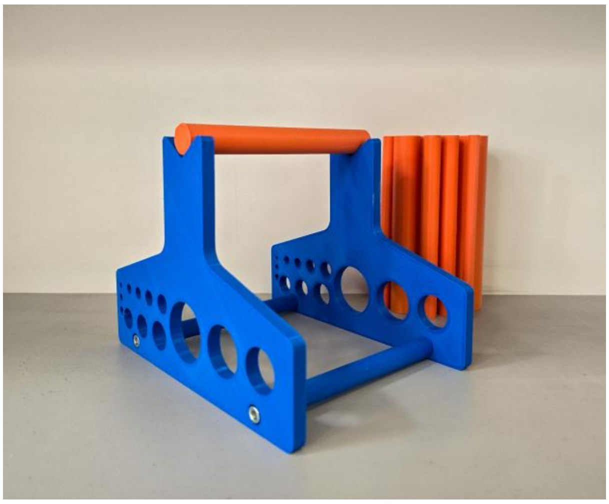

Fig. 6. Bending device

2.5 GOM Aramis 5M

GOM ARAMIS 5M is a non-contact optical measurement system that works on the principle of digital image correlation (DIC). The device uses two cameras with a resolution of 2050 × 2448 pixels to record and track a stochastic speckle pattern applied to the test specimen's surface during loading. This allows it to determine 3D displacements, deformations, and strain distributions across the entire surface. The typical image refresh rate is 15 Hz, which can be increased to over 25 Hz at reduced resolution [41,42].

The quality of the speckle pattern is decisive for the measurement results. Surface preparation (cleaning, priming, painting) and selecting the right paint are crucial for reducing noise and improving measurement reliability. In particular, the characteristic speckle feature size should be matched to the correlation subset (facet) size, since a speckle that is too fine relative to the subset increases interpolation bias, whereas an overly coarse speckle reduces spatial resolution; both degrade the correlation accuracy [2,3]. With optimal parameters, ARAMIS 5M delivers more accurate and reproducible results [43]. Figure 7 shows the measured characteristic speckle dot size that is quantitatively related to the subset size from the ARAMIS software.

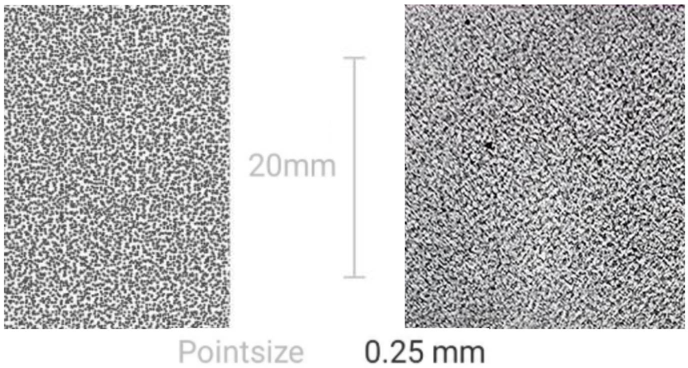

Fig. 7. Speckle pattern size: Sample from ARAMIS (left side), sample from measurement (right side)

2.6 Erichsen Test Configuration and DIC Validation

To examine the deformation of the leather samples, the Erichsen test was used in accordance with ISO 20482:2013, Metallic materials – Sheet and strip – Erichsen cupping test, which ensures slow, well-controlled loading and high elongation of the test specimens, allowing the behavior of the paint to be easily observed. The experiments were carried out using a hydraulic Erichsen device with a 20 mm diameter stamp and a fixed crimp, the clamping force of which was determined by test measurements to ensure that the sample did not slip or become damaged. The deformation was recorded by a GOM ARAMIS 5M DIC system installed above the test area, and the measurement results were compared with the device's displacement measurements to validate the data. During processing, special attention was paid to evaluating the quality of the 3D point cloud generated from the painted surface, as incomplete or broken patterns can cause data loss, impair the evaluability of measurement results, and ultimately reduce measurement accuracy. Figure 8 illustrates the experimental setup [44].

3. Results and Discussion

The current section presents the test results. Samples S1 and S2 were prepared as described in Section 2. For sample S3, the door trim from a dismantled vehicle was examined during the research. It was not possible to cut out test specimens of the appropriate size from this element, so the five paints that performed best in the bending test performed on the S1 samples were tested on the available flat surfaces. This opportunity allowed us to test automotive upholstery in its installed state.

3.1 Results of Paint Performance Tests

Accurate and reliable DIC test results are determined well before the measurement begins and must be ensured beforehand. The preparatory steps for the measurement, especially the proper surface preparation, fundamentally determine the quality of the results. The following subsections present the results of the paint tests, Erichsen test, and DIC measurements, and the conclusions drawn from them are discussed in Section 4.

Fig. 8. The experimental setup

3.1.1 Thickness Measurement Results

Table 3 shows the results of thickness measurements taken with the Elcometer 112Al wet film comb gauge on sprayed and brush-applied paint samples. The values were recorded with a wet-film comb gauge and therefore represent wet-film thickness, which is inherently greater than the cured dry-film thickness; they are reported here for comparative purposes only.

The "-" shown on the S3 samples indicates that no test was performed with that paint, since the samples were prepared with the five selected paints. The "x" means that no DIC test was performed with the black paints marked in this way because, as mentioned earlier, it was not physically possible to cut out test specimens of the appropriate size from the vehicle door, so they could not be fixed in the Erichsen machine for the DIC test. The results show that the paint applied with a brush (P9) produced thicker results, due to the application method. The other paints provided nearly identical coverage in a thin layer. It can also be observed that the layer was slightly thicker on the S2 felt sample, due to the material's structure and "hairy" surface.

Table 3
The measurement result of the paint layer thickness

ID	Avg. Thickness [µm]		
	S1	S2	S3
P9	500	550	450
P10	300	350	350
P11	225	300	x
P12	175	225	200
P13	200	225	-
P14	150	175	x
P15	125	100	100
P16	175	150	x
P17	225	300	-
P18	275	250	-
P19	175	150	x
P20	200	250	-
P21	150	225	x
P22	175	275	150
P23	225	200	x
P24	150	175	-

3.1.2 Touch Test

The Touch Test results clearly show that drying times vary significantly between different paints and samples (S1–S3). On sample S1, most paints dried within 5–10 minutes, with two notable exceptions: P22 – 21.67 minutes; P24 – 35 minutes. In the case of sample S2, drying times were generally longer, with high values observed for several paints (e.g., P9 – 33.33 minutes; P15 – 50 minutes; P24 – 48.33 minutes). In the case of sample S3, the tests were performed with 5 paints, and the results show that, in several cases, the drying times of the paints were the same as those of sample S1 or fell between the results of samples S1 and S2. In the case of the S2 samples, the longer drying time is due to the sample material: the felt can absorb the paint, and the "sponge" effect can take hold, resulting in a longer drying time.

Table 4 shows the results of the Touch Test. The table shows the average drying times for each paint.

Table 4
Results of the Touch Test

ID	Avg. Drying Time [min]		
	S1	S2	S3
P9	10	33.33	15
P10	5	10	5
P12	5	5	5
P13	5	10	-
P15	10	50	10
P17	5	5	-
P18	5	30	-
P20	6.67	15	-
P22	21.67	10	15
P24	35	48.33	-

3.1.3 Print-Free Test

Table 5 shows the results of the Print-Free Test performed on samples S1, S2, and S3. The measurements were performed for each paint and sample under different loads (20 g, 200 g, 500 g, and 1000 g) and repeated three times. The test began 30 minutes after painting, or when the Touch Test results allowed.

The results show that several paints (e.g., P10, P13, P15, P17, P18, P20, and P24) passed all four weight loads on the first attempt, indicating they passed the test at the start.

The difference is most noticeable in the P12 and P22 paints: at higher loads (200–1000 g), drying times were longer, especially on the S2 and S3 samples, where they reached 60–65 minutes. These paints therefore have longer drying times, which is important information for planning future experiments, as it means waiting up to several hours before starting a measurement.

No evaluable data are available for the P9 paint, as it did not pass the test even after hours under the smallest load of 20 g. This is probably because the paint is a thick, washable textile paint that can only be applied in thicker layers when brushed on, significantly increasing drying time.

Table 5
Results of the Print-Free Test

ID	Avg. Print-Free Drying Time [min]											
	S1				S2				S3			
	20	200	500	1000	20	200	500	1000	20	200	500	1000
P9	-	-	-	-	-	-	-	-	-	-	-	-
P10	30	30	30	30	30	30	30	30	30	30	30	30
P12	30	65	50	45	30	30	45	30	45	55	65	60
P13	30	30	30	30	30	30	30	30	-	-	-	-
P15	30	30	30	30	30	30	30	30	30	30	40	30
P17	30	30	30	30	30	40	40	30	-	-	-	-
P18	30	30	30	30	40	30	30	30	-	-	-	-
P20	30	30	30	30	30	30	30	30	-	-	-	-
P22	30	30	30	30	40	40	30	30	30	45	40	30
P24	30	30	30	30	30	30	30	30	-	-	-	-

3.1.4 Cross-Cut Test

The results of the Cross-Cut test are summarized in Table 6. The degree of damage to the painted surface was classified into one of the categories ranging from 0 to 5 specified in the standard, where 0 represents a completely undamaged coating, and 5 represents significant or complete detachment. When the required category could not be clearly determined, two values were recorded. In Table 6, the columns labelled Specimen 1–3 correspond to the three replicate test specimens prepared for each material, and a dual entry (e.g., 2–3) denotes a borderline result falling between two adjacent classification grades. The felt material (S2) was excluded from the cross-cut evaluation, because the lattice-cut method is intended for coating films on firm substrates rather than for soft, fibrous textiles; it is therefore omitted from Table 6. In the S1 samples, the different paints behaved differently along the cuts. Some samples, such as P13 (Figure 9(a)), P17, and P24, showed good adhesion (low values), while others, such as P22, showed significant detachment (Figure 9(b)).

Another problem is that when the adhesive tape is pulled off, it is not the coating that comes off the substrate; rather, the fibers themselves often tear out of the material, distorting the result (Fig. 11(b)). For all these reasons, the cross-cut test cannot be performed on felt or felt-like materials, so the results are not included in the table. However, due to the material's absorbency, the paint is unlikely to peel off; this must be taken into account during the bending test.

Table 6
Results of the Cross-Cut Test

ID	Classification of the appearance			
	S1			S3
	Specimen 1	Specimen 2	Specimen 3	Specimen 1
P9	3	2	3	3
P10	1	2–3	1	1
P12	2	1	1–2	1
P13	0	0	0	-
P15	4	3	3	1
P17	1	1	1	-
P18	2–3	4	2	-
P20	2	2	2–3	-
P22	4	4–5	4–5	2
P24	1	1	1	-

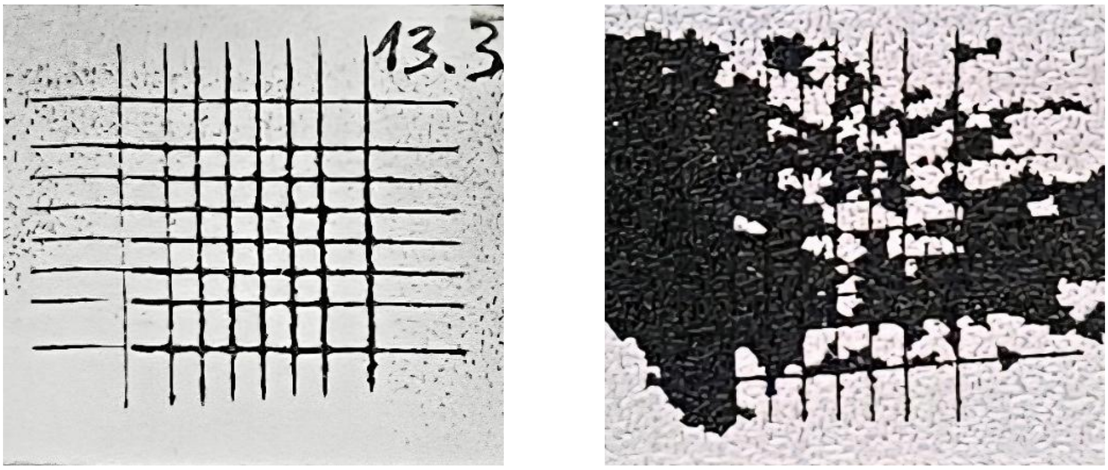

(**a**) (**b**)

Fig. 9. Results of sample S1 with paints: (a) P13 and; (b) P22

For S3 samples, the five paints tested typically showed values equal to or lower than those of the other two. Figure 10 illustrates the results of the Cross-Cut Test for P9 and P12 paints.

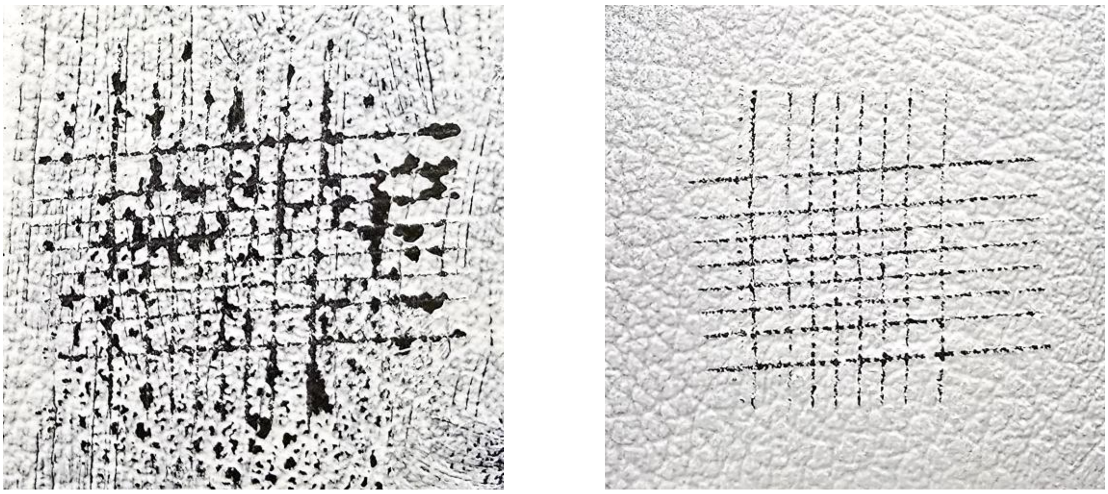

(**a**) (**b**)

Fig. 10. Results of sample S3 with paints: (a) P9 and (b) P12

The Cross-Cut adhesion test cannot be interpreted or reliably applied to the S2 felt sample. This is because the fabric's surface is not homogeneous; it consists of loose fibers to which the coating can only partially adhere. During cutting, the blade does not form a regular grid pattern but rather splits or displaces the fibers, leaving the cuts practically invisible (Figure 11(a)), so the test does not measure the actual adhesion of the paint.

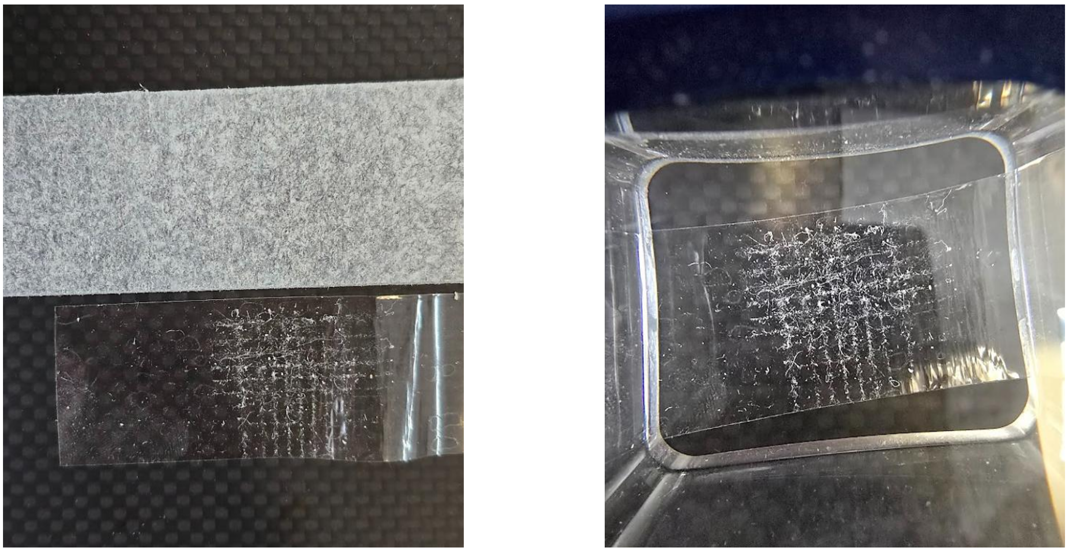

(**a**) (**b**)

Fig. 11. Result of Cross-Cut Test on sample S2: (a) cuts on the specimen; (b) tape removal result

3.1.5 Bending Test

The results of the bending test are summarized in Table 7, where the symbols have the following meanings: S – separates but no crack, G – good adhesion, and C – cracked. In some cases, the test results fell into more than one category, so these are indicated. The tests clearly show that the different test specimens behaved differently during bending. In the case of the S specimens, the coating partially separated from the synthetic leather, but no cracks formed. The specimens marked with a G value showed strong adhesion, with no cracks or separation observed during bending, and were therefore classified as the best results. The samples marked C showed cracks under bending stress.

For the fabric-based, fibrous S2 samples, the bending test did not yield meaningful results. This is because the coating does not form a homogeneous, closed layer but instead penetrates between the fibers. As a result, bending does not allow for evaluating adhesion between the paint and the substrate, but rather reveals the displacement, deformation, or tearing of the fibers relative to one another. The test, therefore, does not provide information on paint detachment, and the method is meaningless for paint adhesion in this case. Subjective observation indicates that no paint fell off the samples' surfaces when bent, suggesting good adhesion.

As it was not possible to cut out test specimens for the S3 samples, the Bending test could not be performed.

To ensure the completeness of the test series, the behavior of the selected paints under deformation was examined on two samples (S1 and S2). The test was performed using Erichsen testing equipment, which enabled observation of the paints under controlled conditions.

Figure 12 illustrates the differences between the three main categories: the P15 sample is separated but not cracked (S) (Figure 12(a)), the sample P22 showed strong adhesion (G) (Figure 12(b)), while P18 showed cracks during bending (C) (Figure 12(c)).

The Bending Test results showed that the P18 paint cracked on the surface when deformed, which was also confirmed by the Erichsen test (Figure 13(a)). By contrast, Figure 13(b) and (c) present two well-performing combinations—S1: P22_P19 and S2: P9_P19—in which the coating and its speckle pattern remained intact, and the deformation could be tracked uniformly up to 23 mm. The following subsection contains the results.

Table 7
Results of Bending Test

ID	S1					
	After drying ("0 h")			24 h		
	1	2	3	1	2	3
P9	G	G	G	G	G	G
P10	G	C	C	C	C	C
P12	G	C	G	C	C	C
P13	C	C	C	C S	C S	C S
P15	S	G	S	C S	C S	C S
P17	C	C	C	C	C	C
P18	C	C	C	C S	C S	C S
P20	C	C	C	C S	C S	C S
P22	G	G	G	C S	C S	C S
P24	C	C	C	C	C	C

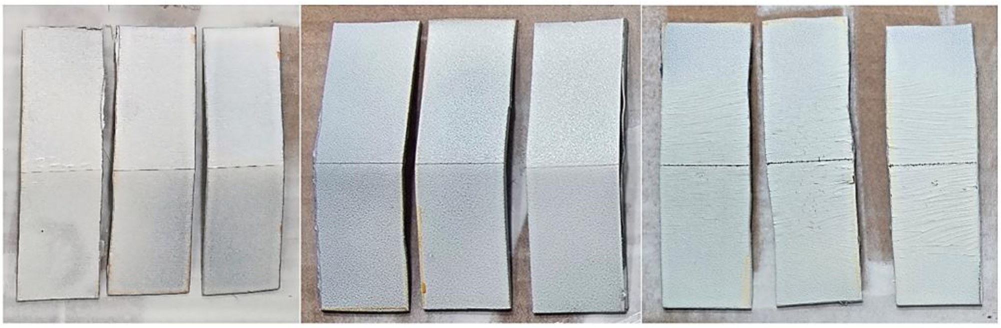

(**a**) (**b**) (**c**)
Fig. 12. Bending test results of sample S1: (a) P15 – separates but no crack (S); (b) P22 – good adhesion (G); (c) P18 – cracked (C)

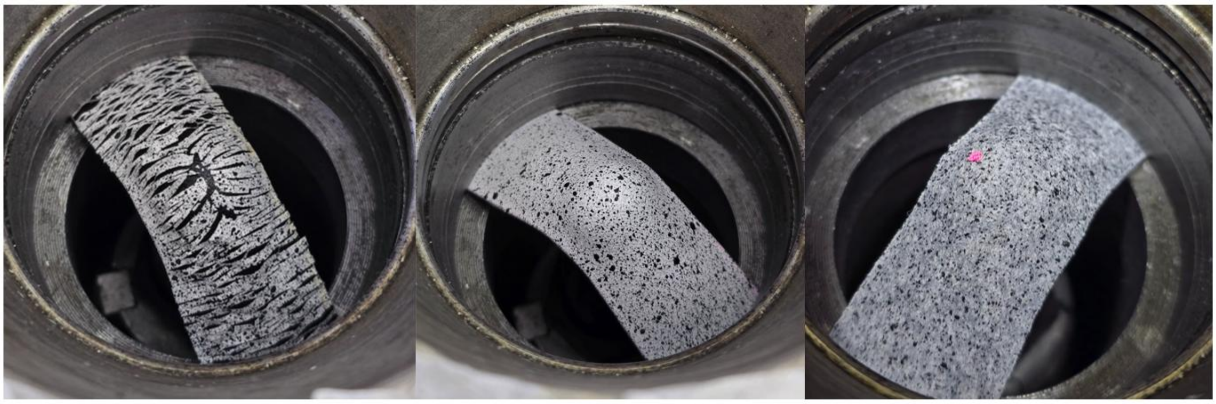

(**a**) (**b**) (**c**)
Fig. 13. Results of Erichsen test: (a) S1: P18_23; (b) S1: P22_P19; (c) S2: P9_P19

3.1.6 Consolidated Evaluation of Paint Performance

Taken together, the four paint-performance tests identify a consistent group of best-performing coatings. Among the light primers, P9 and P22 combined acceptable drying behavior (Sections 3.1.2–3.1.3) with the most favorable cross-cut adhesion (Section 3.1.4) and were classified as good (G) in the bending test (Section 3.1.5); they were therefore selected as the basis for the DIC speckle patterns. P13, P17, and P24 likewise showed good cross-cut adhesion, whereas P18 performed worst overall, cracking under bending and producing discontinuous point clouds in the subsequent DIC measurements. The felt material (S2) absorbed the applied paint and dried slowly, and was unsuitable for the cross-cut test.

3.2 Results of DIC Measurements

The aim of the investigation is to verify the reliability and accuracy of speckle patterns generated by different paints under mechanical loading (Erichsen test).

The current section of the research presents the results of DIC measurements from the Erichsen test. The surface was given a stochastic speckle pattern following the procedure described in Section 2. To further improve measurement accuracy, only the two most effective light paints (P9 and P22) from those proven to be the best in Section 3.1.5 were selected as the basis for the speckle pattern. The speckle pattern created with dark paints (P11, P14, P16, P19, P21, and P23) was applied to this light layer, as shown in Figure 14. In addition to these, P18, one of the worst-performing paints in the Bending Test, was also tested.

(a) **(b)** **(c)** **(d)** **(e)** **(f)**

Fig. 14. Paints used to create the speckle pattern in the case of the S2 and S1 samples, on a P22 base color: (a) P11; (b) P14; (c) P16; (d) P19; (e) P21; (f) P23

The purpose of the measurement is to determine which paint can most accurately reproduce the stamp's displacement, i.e., the length of the actual deformation section within the 33 mm path, which is 23 ± 0.3 mm (the ±0.3 mm indicates the verified stopping accuracy of the equipment). The maximum stamp displacement values obtained with DIC, summarized in Table 8, must be compared to this reference value of 23 ± 0.3 mm. In addition, it is particularly important to determine the level of detail of the point cloud reproduced by each painting process. This is important because where the point cloud is interrupted, there is no measurement data and therefore no result.

Given the surface pattern and texture of the S2 sample, we performed the DIC test without priming or speckle pattern painting. The values in the table were determined as the average of three measurements.

Table 8 shows several interesting findings. Deviations of less than 2% are acceptable, as they are comparable to the equipment's stopping accuracy. It is interesting to note that the white-based felt samples without a pattern (S2) achieved better results than the painted versions. This proves that in DIC tests, if the sample has a pattern in its own material, it can be used effectively even without painting. Errors above 5% confirm the assumption that the paints used for DIC measurements matter, as paint performance strongly influences measurement results.

Table 8
Results of DIC Measurements

ID	Distance from DIC [mm]		Distance from movement [mm]		in Tolerance		% Deviation	
	S1	S2	S1	S2	S1	S2	S1	S2
P9_P11	21.871	22.076	23±0.3	23±0.3	–1.129	–0.924	4.909	4.017
P9_P14	21.851	23.289	23±0.3	23±0.3	–1.149	0.289	4.996	1.256
P9_P16	21.155	22.655	23±0.3	23±0.3	–1.845	–0.345	8.022	1.5
P9_P19	19.185	23.313	23±0.3	23±0.3	–3.815	0.313	16.587	1.361
P9_P21	22.31	23.397	23±0.3	23±0.3	–0.69	0.397	3	1.726
P9_P23	25.387	23.451	23±0.3	23±0.3	2.387	0.451	10.378	1.961
P22_P11	22.915	22.814	23±0.3	23±0.3	–0.085	–0.186	0.369	1.809
P22_P14	22.174	22.574	23±0.3	23±0.3	–0.826	–0.426	3.591	1.852
P22_P16	22.756	22.497	23±0.3	23±0.3	–0.244	–0.503	1.061	2.187
P22_P19	22.958	22.736	23±0.3	23±0.3	–0.042	–0.264	0.183	1.148
P22_P21	22.298	22.752	23±0.3	23±0.3	–0.702	–0.248	3.052	1.078
P22_P23	22.458	23.234	23±0.3	23±0.3	–0.542	0.234	2.356	1.017
P18_P23	22.605	23.419	23±0.3	23±0.3	–0.395	0.419	1.717	1.822
w/o painting	-	23.125	-	23±0.3	-	–0.125	-	0.543

A number of primer-topcoat paint combinations produced deviations above 10% from the 23 mm reference value (for example, several P9- and P22-based combinations on S1). Two distinct mechanisms can give rise to such large deviations, and they must be interpreted differently. The first is physical failure of the paint layer: when a coating cracks, flakes, or detaches during the Erichsen stroke—as observed for the high-detachment combinations in the cross-cut test (Section 3.1.4) and for the cracked panels shown in Figure 13—the speckle carrier is locally destroyed, the surface loses contrast, and the reconstructed 3D point cloud becomes discontinuous, so the last reliably trackable position is reached before the true end of the stroke. The second is a digital image correlation tracking error in the absence of physical failure: a speckle that is too fine, too sparse, or of insufficient contrast relative to the subset (facet) size degrades subset matching and can cause premature correlation loss even though the coating remains intact [2,3]. In the present measurements, the largest deviations occur for combinations that also exhibited poor adhesion and visible cracking, which indicates that physical paint failure—rather than pure tracking error—is the dominant cause in those cases.

After reviewing the measurement results, we are convinced that this large percentage deviation is caused by defects in the above-mentioned paint combinations. We have also observed similar defects during measurements performed on sheet materials.

The color maps in Figures 15 and 16 clearly illustrate the results of the DIC examination. On sample S1, the speckle patterns produced with paints applied to the properly adhering P9 and P22 primers resulted in fairly continuous color maps with minimal gaps, i.e., point clouds (Figures 15 and 16). In these cases, the maximum stamp displacement values can be clearly determined. Some of the continuity errors detected are merely the result of black paint spots dripping during painting.

In addition to the two best-performing primer paints on the S1 sample, P18, the previously worst-performing paint, was also subjected to DIC testing. This was necessary to clearly demonstrate the dangers of using paint unsuitable for DIC measurement. Figure 17 shows that the paint separates from the surface, the point cloud disintegrates, and the measurement cannot be evaluated; there is no data to provide a result.

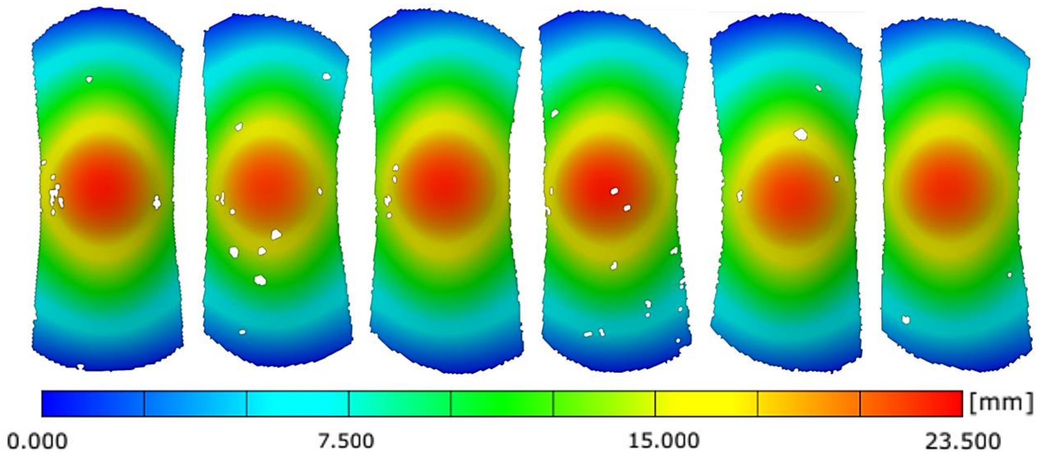

Fig. 15. Results of DIC Measurements on sample S1 with P22 base paint: P11, P14, P16, P19, P21, P23

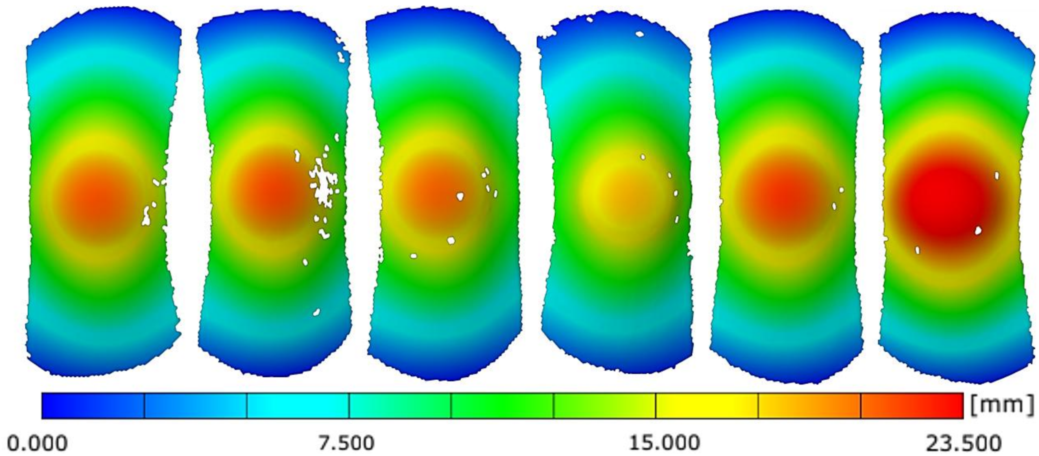

Fig. 16. Results of DIC Measurements on sample S1 with P9 base paint: P11, P14, P16, P19, P21, P23

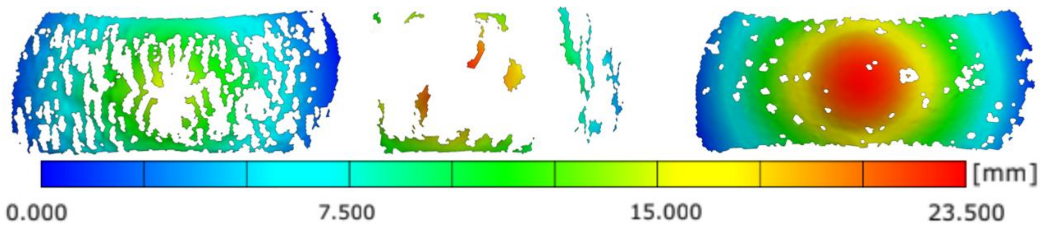

Fig. 17. Results of DIC measurements: for S1_P18_P23 not at maximum punch stroke, and for S1_P18_P23 and S2_P18_P23 at maximum punch stroke

When examining the S2 samples (Figures 18 and 19), it was found that the consistency of the measurement results was worse than that of S1. In several cases, especially when using the P22 base paint, less homogeneous color maps were observed. However, the maximum displacements are clearly visible. Due to the surface's natural texture, it was possible to perform DIC analysis on the S2 sample without painting, but the results were extremely incomplete, with measurement data missing at the material's maximum displacement. However, despite its limitations, this material can be measured without painting. As shown in Table 9, the table indicates the percentage deviation of the point cloud of the final measured state from that of the initial state for each paint-sample combination.

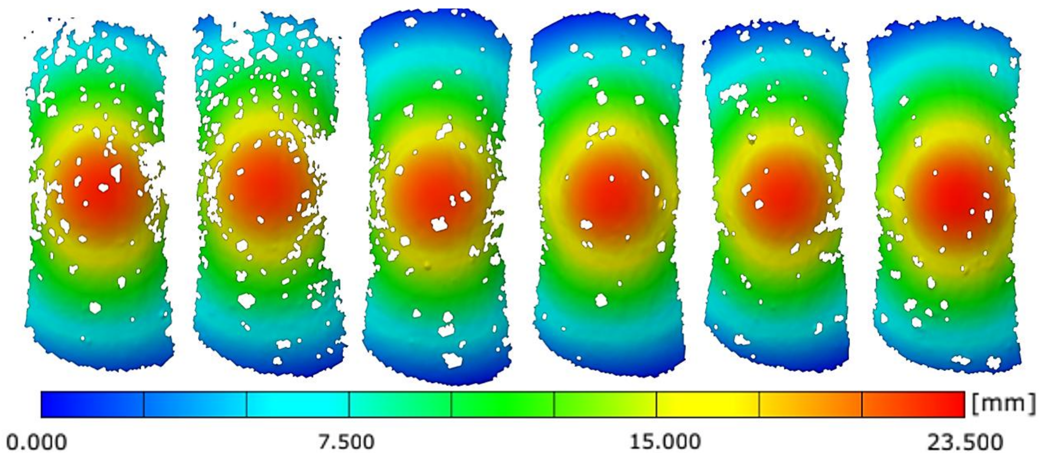

Fig. 18. Results of DIC Measurements on sample S2 with P22 base paint: P11, P14, P16, P19, P21, P23

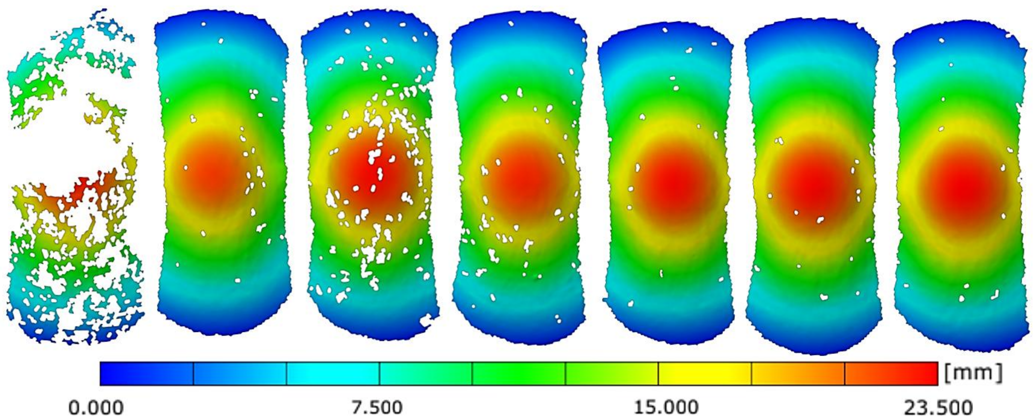

Fig. 19. Results of DIC Measurements on sample S2 without painting and with P9 base paint: P11, P14, P16, P19, P21, P23.

Table 9
Results of point-cloud continuity

ID	% Deviation	
	S1	S2
P9_P11	2.07	1.917
P9_P14	2.581	6.6
P9_P16	1.048	2.878
P9_P19	1.212	1.475
P9_P21	0.976	1.432
P9_P23	2.267	1.696
P22_P11	0.62	9.566
P22_P14	0.855	12.946
P22_P16	1.476	7.244
P22_P19	1.787	2.793
P22_P21	1.584	4.557
P22_P23	1.394	3.607
P18_P23	85.078	4.766
w/o	-	50.131

4. Conclusions

Based on the Touch Test results, sample S1 had the fastest drying time, while sample S2 typically showed a significantly longer drying time. Sample S3 provided intermediate results; however, data are not available for all paints. P24 exhibited an exceptionally long drying time on sample S2 and was more sensitive to its surface characteristics. In the Print-Free Test, most paints delivered fast, stable drying across the entire load range, while P12 and P22 showed longer drying times at higher loads.

Based on the adhesion test results (Cross-Cut and Bending Tests), the S1 substrate provided the best comparable basis, as the characteristics of the S2 textile structure distorted the measurements. For S3, the tests could only be carried out to a limited extent. According to the bending tests, P22 and P9 paints showed the best adhesion and elasticity, while several other paints (e.g., P18) were prone to cracking. This test also confirmed that selecting a suitable primer is crucial for forming durable speckle patterns that can mediate shape changes.

The results of the Erichsen tests showed that certain paints (e.g., P18) are unable to withstand shape changes at high elongation, as they crack and peel from the surface. In contrast, the P9 and P22 primer paints (together with the spot pattern) provided good stability and enabled accurate tracking of the deformation.

It can be concluded that the best results were observed with sample S1, with both high-performance primer paints showing fairly consistent results. In the case of sample S2, the results were more significantly influenced by which primer paint or black paint was applied. When P9 paint was utilized as a base, more continuous point cloud results were obtained. The point clouds with the fewest deficiencies were S2_P9_P19 and S2_P9_P23. P18 exhibited the weakest performance, leading to measurement errors and discontinuous deformation fields due to surface cracks. The DIC measurements were also validated against Erichsen measurements; the best-performing paints showed a displacement deviation of less than 2%. A further result is that felt samples can be measured even without a spot pattern, but only with limitations and poor-quality point clouds.

The research results confirmed that the quality of the substrate surface, the base paint, and the speckle pattern fundamentally determine the measurement results. This supports the conclusion that, with the right choice of paint, commercially available sprays are suitable for DIC measurements, but care must be taken when selecting paints, as not all are suitable for this purpose. This study provides results to aid in this selection.

Several limitations must be acknowledged. The investigation focused on a limited range of synthetic leathers and paint brands, and the results may differ with other materials or under varying environmental conditions, such as humidity and temperature fluctuations. Certain mechanical tests, including bending and cross-cutting, could not be meaningfully applied to the felt substrate because of its fibrous structure. Furthermore, the long-term durability of the coatings under ultraviolet exposure or cyclic mechanical loading was not assessed and could influence performance over time.

Future research should therefore extend testing to a wider selection of automotive interior materials, including multilayer composites and complete seat assemblies. It should evaluate the effects of environmental aging, temperature-humidity cycling, and UV exposure on paint adhesion and DIC accuracy. Automated or ink-based speckle application techniques warrant investigation to achieve more consistent pattern quality. At the same time, advanced image analysis methods could help directly link speckle size and distribution to measurement noise and precision. The exploration of environmentally friendly, low-VOC coatings and primers is also recommended to support sustainable industrial practices.

Taken together, these findings provide a practical reference for preparing synthetic leather surfaces for DIC and establish a solid foundation for further improvements in surface preparation and measurement reliability.

Acknowledgement
The authors acknowledge the technical help of the research team they belong to, namely the 'SZE-RAIL' at SIU.

Conflicts of Interest
The authors declare no conflicts of interest.

Declaration on the Use of Artificial Intelligence Tools
During the preparation of this manuscript, the author used Grammarly and DeepL solely for language editing and proofreading.

References
Lecompte, D., Smits, A., Bossuyt, S., Sol, H., Vantomme, J., Van Hemelrijck, D., & Habraken, A. M. (2006). Quality assessment of speckle patterns for digital image correlation. *Optics and Lasers in Engineering*, 44(11), 1132–1145. https://doi.org/10.1016/j.optlaseng.2005.10.004
Pan, B., Lu, Z., & Xie, H. (2010). Mean intensity gradient: An effective global parameter for quality assessment of the speckle patterns used in digital image correlation. *Optics and Lasers in Engineering*, 48(4), 469–477. https://doi.org/10.1016/j.optlaseng.2009.08.010
Crammond, G., Boyd, S. W., & Dulieu-Barton, J. M. (2013). Speckle pattern quality assessment for digital image correlation. *Optics and Lasers in Engineering*, 51(12), 1368–1378. https://doi.org/10.1016/j.optlaseng.2013.03.014
Taran, I., Karsybayeva, A., Naumov, V., Murzabekova, K., & Chazhabayeva, M. (2023). Fuzzy-logic approach to estimating the fleet efficiency of a road transport company: A case study of agricultural products deliveries in Kazakhstan. *Sustainability*, 15(5), 4179. https://doi.org/10.3390/su15054179
Oliskevych, M., Taran, I., Volkova, T., & Klymenko, I. (2022). Simulation of cargo delivery by road carrier: Case study of the transportation company. *Naukovyi Visnyk Natsionalnoho Hirnychoho Universytetu*, (2), 118–123. https://doi.org/10.33271/nvngu/2022-2/118
Novytskyi, O., Taran, I., & Zhanbirov, Z. (2019). Increasing mine train mass by means of improved efficiency of service braking. *E3S Web of Conferences*, 123, 01034. https://doi.org/10.1051/e3sconf/201912301034
Jing, L., Guo, N., Xu, H., Jiang, J., Zhang, T., & Chen, N. (2017). Tensile characteristics of flexible PU-coated multi-axial warp-knitted fabrics. *Journal of Industrial Textiles*, 47(1), 38–56.
Lomov, S. V., Boisse, P., Deluycker, E., Morestin, F., Vanclooster, K., Vandepitte, D., Verpoest, I., & Willems, A. (2008). Full-field strain measurements in textile deformability studies. *Composites Part A: Applied Science and Manufacturing*, 39(8), 1232–1244. https://doi.org/10.1016/j.compositesa.2007.09.014
Mitrović, N., Mitrović, A., & Reljić, M. (2021). Strain measurement of medical textile using 2D digital image correlation method. In *Experimental and Computational Investigations in Engineering* (Notes in Networks and Systems, Vol. 153, pp. 447–464). Springer. https://doi.org/10.1007/978-3-030-58362-0_26
He, R., Sun, X., Wu, Y., Tang, G., & Carvelli, V. (2021). Biaxial tearing properties of woven coated fabrics using digital image correlation. *Composite Structures*, 272(10), 114206. https://doi.org/10.1016/j.compstruct.2021.114206
Zhang, L., Zhang, Y., Zhao, Q., Xu, J., & Xue, J. (2020). Shape effect analysis of the mechanical properties of PVC-coated fabrics under off-axis tension. *Advances in Materials Science and Engineering*, 2020, 9634120. https://doi.org/10.1155/2020/9634120
Xu, S., Xia, Z., Yu, T., Zhang, Y., Xu, J., Xu, C., & Sheng, M. (2025). Off-axial tensile properties and failure analysis of PVC-coated fabric with multiple-layer welded seam. *Journal of Industrial Textiles*, 55. https://doi.org/10.1177/15280837251359018
Meyer, M., Dietrich, S., Schulz, H., & Mondschein, A. (2021). Comparison of the technical performance of leather, artificial leather, and trendy alternatives. *Coatings*, 11(2), 226. https://doi.org/10.3390/coatings11020226
Lee, J., Gu, C.-Y., Chang, J., Cho, E. H., Kim, T.-S., & Choi, K. C. (2024). Analytic modeling and validation of strain in textile-based OLEDs for advanced textile display technologies. *npj Flexible Electronics*, 8(1), 73. https://doi.org/10.1038/s41528-024-00361-9
Khennouf, D., Dulieu-Barton, J. M., Chambers, A. R., Lennard, F. J., & Eastop, D. (2008). Application of digital image correlation to deformation measurements in textiles. In *Proceedings of Photomechanics 2008: International Conference on Full-Field Measurement Techniques and their Applications in Experimental Solid Mechanics*. Loughborough, UK.

Williams, H. R., Lennard, F., Eastop, D., Dulieu-Barton, J. M., & Chambers, A. R. (2009). Application of digital image correlation to tapestry and textile condition assessment. In *Proceedings of AIC Textile Specialty Group* (pp. 156–170). Los Angeles, USA.

Kuchak, A. J. T., Marinković, D., & Zehn, M. (2020). Finite element model updating – Case study of a rail damper. *Structural Engineering and Mechanics*, 73(1), 27–35. https://doi.org/10.12989/sem.2020.73.1.027

Kuchak, A. J. T., Marinković, D., & Zehn, M. (2021). Parametric investigation of a rail damper design based on a lab-scaled model. *Journal of Vibration Engineering & Technologies*, 9(1), 51–60. https://doi.org/10.1007/s42417-020-00209-2

Evans, S. L., & Holt, C. A. (2009). Measuring the mechanical properties of human skin in vivo using digital image correlation and finite element modelling. *The Journal of Strain Analysis for Engineering Design*, 44(5), 337–345. https://doi.org/10.1243/03093247JSA488

Savić, V., & Hector, L. (2013). Tensile material properties of fabrics for vehicle interiors from digital image correlation. *SAE Technical Paper*, 2013-01-1422. https://doi.org/10.4271/2013-01-1422

Siyao, M., Liu, S., Peihua, Z., & Hairu, L. (2020). Functional investigation on automotive interior materials based on variable knitted structural parameters. *Polymers*, 12(11), 2455. https://doi.org/10.3390/polym12112455

Ujević, D., Kovačević, S., Wadsworth, L. C., Schwarz, I., & Brlobašić Šajatović, B. (2009). Analysis of artificial leather with textile fabric on the backside. *Journal of Textile and Apparel, Technology and Management*, 6, 1–9.

Havelka, A., Glombíková, V., Komárková, P., & Chotěbor, M. (2017). The study of fabric performance for car seats. *Tekstilec*, 60(3), 235–242. https://doi.org/10.14502/Tekstilec2017.60.235-242

Sheilla, S., Patrícia, Y., João, M., Luiz, H., Eloy, M., & Paulo, N. (2019). Increased resistance to dirt and staining on artificial leather. *SAE Technical Paper*, 2019-36-0123. https://doi.org/10.4271/2019-36-0123

Lei, Z. (2020). Study on test of color fastness to rubbing of textiles. *IOP Conference Series: Materials Science and Engineering*, 793, 012017. https://doi.org/10.1088/1757-899X/793/1/012017

Kumpikaitė, E., Tautkutė-Stankuvienė, I., Milašienė, D., & Petraitienė, S. (2022). Analysis of color fastness and shrinkage of dyed and printed linen/silk fabrics. *Coatings*, 12(3), 408. https://doi.org/10.3390/coatings12030408

Wang, Y., & Zhao, J. (2019). Facile preparation of slag or fly ash geopolymer composite coatings with flame resistance. *Construction and Building Materials*, 203, 655–661. https://doi.org/10.1016/j.conbuildmat.2019.01.097

Trung, T. N. (2022). Improvement of environmentally-friendly alkyd composite coating with graphene oxide. *Malaysian Journal on Composites Science and Manufacturing*, 7, 1–10. https://doi.org/10.37934/mjcsm.7.1.110

Brillux Industrial Coatings. (2015). A more efficient production process. *IST International Surface Technology*, 8, 13. https://doi.org/10.1007/s35724-015-0564-0

Todorov, N., Yaneva, K., & Denev, Y. (2018). Alkyd resins based on glycerol phase from rapeseed oil biodiesel production. *Annual of Assen Zlatarov University*, 47, 50–55.

Butschle, M., Schackmann, M., & Dam-Johansen, K. (2024). Challenging toxic tin catalysts in polyurethane coatings through serendipity. *Journal of Coatings Technology and Research*, 21(5), 1857–1865. https://doi.org/10.1007/s11998-024-00945-0

Hou, X., Ou, J., Li, C., Hu, Y., Wang, F., Fang, X., Li, W., & Amirfazli, A. (2025). Electrostatic spraying of zinc carbonate hydroxide-infused ethylene-tetrafluoroethylene powders: A thermally-induced, VOC-free antibacterial superhydrophobic coating. *Colloids and Surfaces A: Physicochemical and Engineering Aspects*, 705, 135569. https://doi.org/10.1016/j.colsurfa.2024.135569

Barbu, A., Feier, A. I., Petzek, E., & Gheorghe, M. (2025). Investigation of a composite material painting method: Assessment of the mixture curing of organic coatings. *Processes*, 13(8), 2394. https://doi.org/10.3390/pr13082394

International Organization for Standardization. (2019). *ISO 2808:2019 Paints and varnishes—Determination of film thickness*.

International Organization for Standardization. (1984). *ISO 3270:1984 Paints and varnishes and their raw materials — Temperatures and humidities for conditioning and testing*.

International Organization for Standardization. (2012a). *ISO 9117-6:2012 Paints and varnishes—Drying tests—Part 6: Print-free test*.

International Organization for Standardization. (2012b). *ISO 9117-5:2012 Paints and varnishes—Drying tests—Part 5: Modified Bandow-Wolff test*.

International Organization for Standardization. (2020). *ISO 2409:2020 Paints and varnishes—Cross-cut test*.

International Organization for Standardization. (2011). *ISO 1519:2011 Paints and varnishes—Bend test (cylindrical mandrel)*.

International Organization for Standardization. (2023). *ISO 1518-1:2023 Paints and varnishes—Determination of scratch resistance—Part 1: Constant-loading method*.

Acciaioli, A., Lionello, G., & Baleani, M. (2018). Experimentally achievable accuracy using a digital image correlation technique in measuring small-magnitude (<0.1%) homogeneous strain fields. *Materials*, 11(5), 751. https://doi.org/10.3390/ma11050751

Nemes, V., Szalai, S., Szívós, B. F., Sysyn, M., Kurhan, D., & Fischer, S. (2025). Deformation characterization of glass fiber and carbon fiber-reinforced 3D printing filaments using digital image correlation. *Polymers*, 17(7), 934. https://doi.org/10.3390/polym17070934

Szalai, S., Szívós, B. F., Kurhan, D., Németh, A., Sysyn, M., & Fischer, S. (2023). Optimization of surface preparation and painting processes for railway and automotive steel sheets. *Infrastructures*, 8(2), 28. https://doi.org/10.3390/infrastructures8020028

International Organization for Standardization. (2013). *ISO 20482:2013 Metallic materials—Sheet and strip—Erichsen cupping test*.